Edelweiss Applied Science and Technology
ISSN: 2576-8484
Vol. 8, No. 6, 1554-1565
2024
Publisher: Learning Gate
DOI: 10.55214/25768484.v8i6.2273

Identification of diffusion interlayers of dissimilar welds under static tension by acoustic emission method

V.A. Barat[1,2*], S.V. Ushanov[1], E.A. Lepsheev[1,2], G.V. Sviridov[1], N.V. Lavrik[1]
[1]Moscow Power Engineering Institute, 111250, Moscow, Krasnokazarmennaya st. 17; BaratVA@mpei.ru (V.A.B.)
[2]LLC "INTERUNIS-IT", 111024, Moscow, Shosse Entuziastov st, 20B;
UshanovSV@mpei.ru (S.V.U.), LepsheevYA@mpei.ru (E.A.L.), SviridovGeorB@mpei.ru (G.V.S.), LavrikNV@mpei.ru (N.V.L.).

Abstract: The paper studies the possibility of carbide and decarburized ferrite interlayers detection formed during the production and operation of dissimilar welded joints of austenitic to pearlitic steels. Diffusion interlayers may be interpreted as welded joint microstructure defects, since their formation can cause premature failure of the product under high-temperature operation conditions. In addition, with a certain chemical and structural-phase composition of the welded metals, brittle interlayers formation and development of cracks in the weld zone may be occurred. To identify diffusion interlayers, the acoustic emission (AE) method is used in this research. Specimens cut from welded joints were tested by tension until rupture with simultaneous recording of AE signals. Based on the research results, particular AE data signatures corresponding to the specimens with diffusion interlayers were identified. The main feature indicating the presence of diffusion interlayers is an increase in the amplitudes of AE impulses and AE activity at a stress value of 300 MPa, corresponding to the ultimate strength of the ferrite phase.

Keywords: *Acoustic emission, Diffusion interlayers, Dissimilar welds.*

1. Introduction

Current trends in improving industrial products and structures lead to increased requirements for the applied structural materials and technologies for their processing. Combined structures formed by welding dissimilar or cladding materials are increasingly used. They are used in cases where operating conditions (temperature, environment, mechanical load) differ for different parts of the structure.

When welding, heat treating, or operating dissimilar welded joints at high temperatures, interlayers may form in the fusion zones and heat-affected zones due to the diffusional redistribution of chemical elements contained in base and filler materials. In case of fusion welding of dissimilar steels, the formation of diffusion interlayers is associated with the carbon migration, which forms interstitial solid solutions with iron [1]. As the temperature and operating period of welded joints at high temperatures increase, these processes occur even more intensively; therefore, in dissimilar steels welded joints, decarburized interlayers and interlayers with increased carbide content are often observed near the fusion line [2]. The sizes of such interlayers are largely determined by applied welding technology and operating conditions of the welded joint, which affect the intensity of physical processes occurring at the phase boundary [3].

Diffusion interlayers can form not only in welded joints obtained by fusion but also during pressure welding or cladding [4]. In particular, studies [5, 6] describe cases of diffusion interlayer formation in multi-layered intermetallic composites obtained by explosive welding. Diffusion interlayers form during the heat treatment stage, and their thickness depends on the process

* Correspondence: BaratVA@mpei.ru

temperature and duration. The formation of diffusion interlayers is also noted in powder materials welding joints [7], as well as on the fusion lines of substrates to coatings [8].

Diffusion interlayers can be considered as the welded joint microstructure defects, as their formation can cause premature failure of products under high-temperature operating conditions [1]. Additionally, given certain chemical and structural-phase compositions of the parent metals, conditions can arise for the formation of brittle interlayers and the cracks propagation in the weld zone [9].

The identification of diffusion interlayers is typically carried out through laborious metallographic analysis of etched microsections that allows to determinate the presence of the interlayers, their microstructure and thickness. Additionally, scanning electron microscopy and energy-dispersive X-ray spectroscopy are used to refine the diffusion zones chemical composition. These zones are relatively thin, generally no more than a few hundred microns. To assess the local mechanical properties within the diffusion interlayers, scribing and indentation methods [10] are used. The ultimate tensile strength and yield strength in these regions are determined indirectly based on the hardness values.

Detection of diffusion interlayers by commonly used NDT methods is a complex task, since the interlayer zone does not differ in density, electrical conductivity and acoustic impedance from the weld metal and heat-affected zone. The exception is the acoustic emission (AE) method, which, due to its sensitivity to changes in the microstructure parameters of the materials being tested, allows detection microstructure defects. In particular, authors' preliminary studies have confirmed the feasibility of using the AE method to detect diffusion interlayers in dissimilar welded joints [1].

Research on the patterns of AE signals obtained from dissimilar welded joints of "grade 20" carbon steel and 12Kh18N10T austenitic steel under static tension was conducted in this paper. Both defect-free welded joints (i.e., without diffusion interlayers) and welded joints with diffusion interlayers of varying thickness, produced by MIG-welding, were examined. Based on the analysis of the AE data, taking into account the characteristics of the frequency spectrum, patterns corresponding to the presence of diffusion interlayers in dissimilar welded joints were identified.

2. Materials and Methods of the Research

Dissimilar welded joints of "grade 20" steel (carbon steel with a ferrite-pearlite structure) and 12Kh18N10T steel (an austenitic stainless steel) were the objects of this research. The welded joints were fabricated from sheets of "grade 20" steel and 12Kh18N10T with a thickness of 3 mm. The chemical composition of the 12Kh18N10T and "grade 20" steel is provided in Table 1 and 2. The sheets were cut into strips of 1000 mm long and 200 mm wide and were welded together using MIG welding (Figure 1a).

Welding was performed with a butt joint from both sides, using Sabaros O101 wire as the filler material, which has an austenitic microstructure. The chemical composition of the filler wire is provided in Table 3. The use of Sabaros O101 wire provides the formation of an austenitic microstructure in the weld metal, which is optimal in terms of its mechanical and operational properties. Additionally, the chromium content in the wire contributes to the formation of carbide and decarburized diffusion interlayers during the heat treatment of the welded joints.

Table 1.
Chemical composition of the 12Kh18N10T, % mass.

C	Si	Mn	Ni	S	P	Cr	Cu	Ti	Fe
max 0.12	max 0.8	max 2	9 - 11	max 0.02	max 0.035	17 - 19	max 0.3	0.4-1	~67

Table 2.
Chemical composition of the steel 20, % mass.

C	Si	Mn	Ni	S	P	Cr	Cu	As
0.17-0.24	0.17-0.37	0.35-0.65	Max 0.3	max 0.04	max 0.035	max 0.25	max 0.3	max 0.08

Edelweiss Applied Science and Technology
ISSN: 2576-8484
Vol. 8, No. 6: 1554-1565, 2024
DOI: 10.55214/25768484.v8i6.2273

Table 3
Chemical composition of the Sabaros 0101 filler wire for MIG welding, % mass.

C	Si	Cr	Ni	Mn	Fe
0.10	0.50	19.0	9.0	6.0	Base

The preparation of specimens for tension tests was carried out by laser cutting the welded sheets. The shape and sizes of the test specimens were selected in accordance with the recommendations of tension test standards and the specific requirements of the AE tests being conducted. The width of the specimen gauge section was set at 20 mm to securely attach an AE sensor with a diameter of 15 mm to its surface. The weld was located in the center of the specimen gauge section. The width of the grip section was set at 50 mm to prevent plastic deformation of the 12Kh18N10T steel in the grip area during tension testing (Figure 1b and 1c).

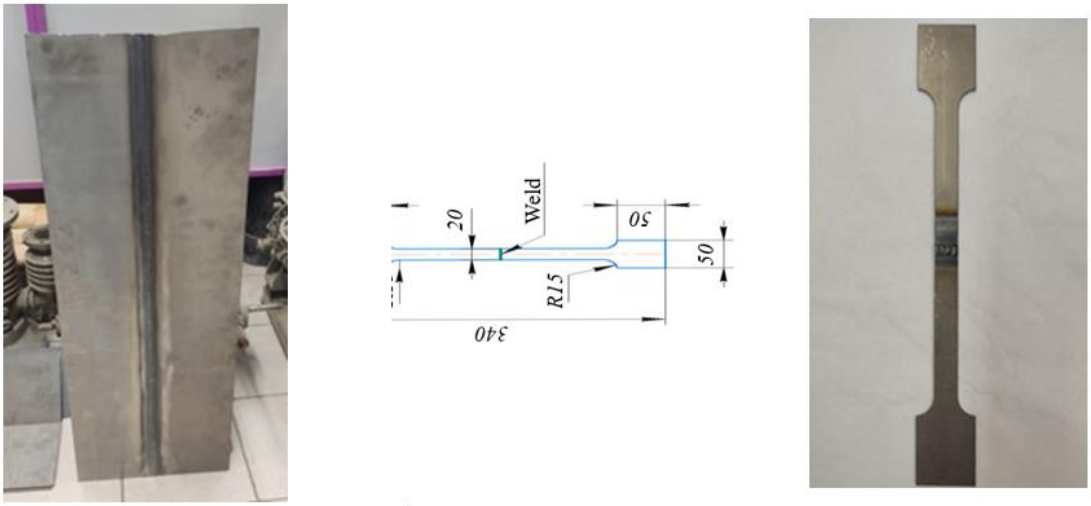

a. b. c.

Figure 1.
Welded sheets made of "grade 20" steel and 12Kh18N10T steel (a), specimen scheme (b), specimens after cut (c).

To form diffusion interlayers in the welded joints, which are usually formed during the long-term operation under high temperatures, a number of the weld specimens were subjected to subsequent heat treatment to simulate the effect of weld long-term operation under high temperatures.

Edelweiss Applied Science and Technology
ISSN: 2576-8484
Vol. 8, No. 6: 1554-1565, 2024
DOI: 10.55214/25768484.v8i6.2273

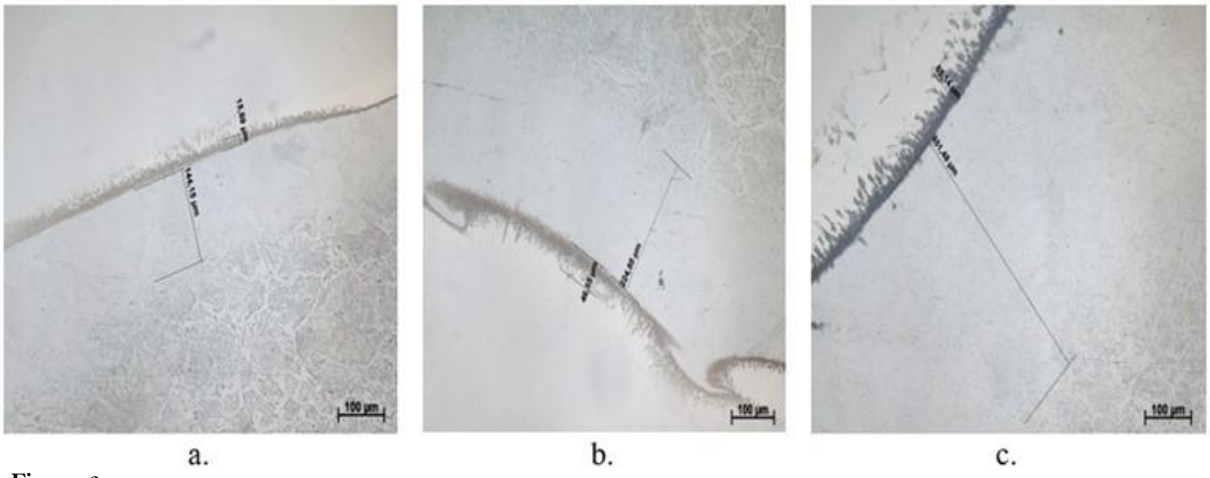

Figure 2.
Image of the "grade 20" steel – weld seam fusion line with diffusion interlayers after heat treatment with 650°C for 1 hour (a), 5 hours (b), 25 hours (c), scaled 200x.

Heat treatment was conducted in a Nabertherm P180 furnace at a temperature of 650°C with different holding times (1 hour, 5 hours, and 25 hours). Different holding times were necessary to form diffusion interlayers of different thicknesses. The average values of the interlayer thicknesses are presented in Table 4. The microstructure of welded joints after heat treatment is shown in Fig.2.

Table 4
Average thickness of diffusion interlayers in welded joints of "grade 20" steel and 12Kh18N10T, obtained by MIG welding, after heat treatment.

No. of heat treatment mode	Time of heat treatment, h	Thickness of decarburized interlayer, μm	Thickness of carbon interlayer, μm
1	1	145	20
2	5	225	45
3	25	600	65

Increasing the heat treatment duration and temperature intensifies the diffusion of carbon from "grade 20" steel into the weld metal, resulting in the thickening of the diffusion interlayers — both carbide and decarburized.

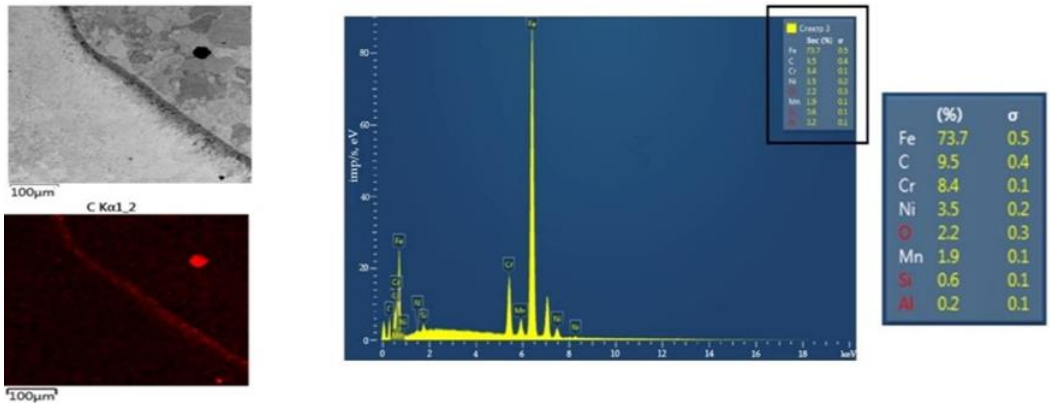

Figure 3.
Image of welded joint near the "grade 20" steel – weld seam fusion line (a), carbon distribution in this area (b), and chemical composition of the carbide interlayer (c).

Edelweiss Applied Science and Technology
ISSN: 2576-8484
Vol. 8, No. 6: 1554-1565, 2024
DOI: 10.55214/25768484.v8i6.2273

Figure 3 shows the microstructure of the "grade 20" steel – weld seam fusion line, the distribution of carbon in this area, and the chemical composition of the carbide interlayer, obtained using scanning electron microscopy (SEM) and energy dispersive X-ray spectroscopy (EDS). It was determined by EDS that the carbide interlayer in the welded joint consists predominantly of chromium carbides.

Tensile tests were conducted at a strain rate of 0.5 mm/min using the Instron 5982 testing machine. A low deformation rate was chosen to identify the patterns of AE generation at different stages of specimen deformation. The experimental setup is shown in Figure 4. The specimens were subjected to testing until failure, with synchronous AE signal recording during the test. Four AE transducers were attached to the specimen: two transducers were attached near the center of the specimen and another two transducers were mounted near the grip sections (Fig. 4b). This scheme of AE transducers mounting allows for the exclusion of acoustic noise associated with the influence of the testing machine grips.

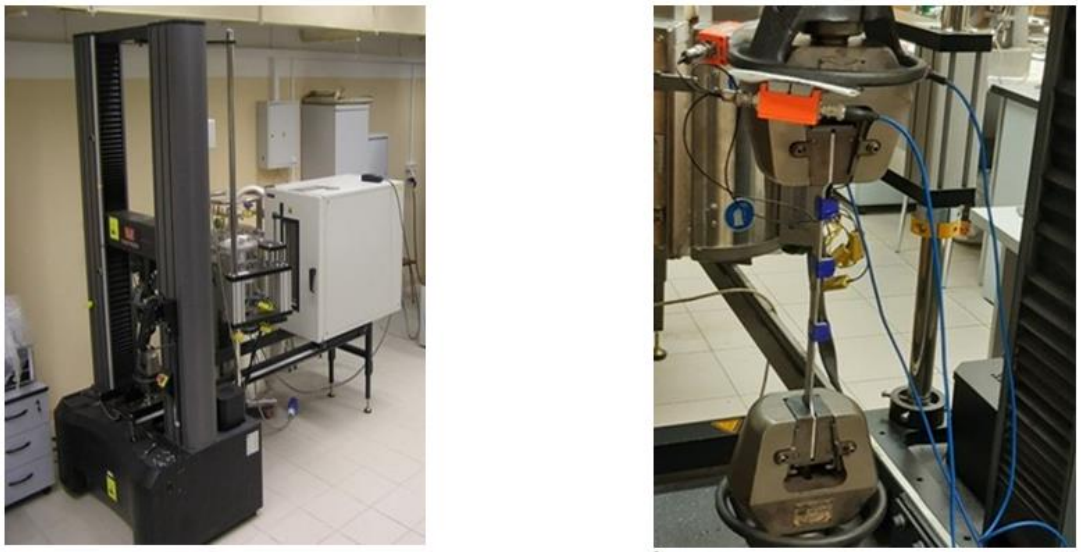

a. b.

Figure 4.
Universal testing machine Instron 5982 (a) and image of a specimen with the attached AE transducers (b).

AE data were recorded using the A-Line 32 system (LLC "INTERUNIS-IT") with PAEF-014 preamplifiers and GT200 AE sensor (LLC "Global Test") with a resonant frequency of 180 kHz. To exclude the noise from the testing machine a bandpass filter with a range of 100–400 kHz, shifted towards higher frequencies, was used. The amplitude discrimination threshold was set at 40 dB.

To determine the mechanical properties of the materials being welded, separate tests were conducted on specimens of the parent materials ("grade 20" steel and 12Kh18N10T steel). The tests were performed at a strain rate of 0.5 mm/min without AE registration.

3. Results

3.1. Tensile Test Results

The results of tensile tests on specimens cut from the parent metals are presented in Table 5. Typical stress-strain curves for specimens made of steel 20 and 12Kh18N10T steel are shown in Fig. 5a. The diagrams and the table indicate that the yield stress values of 12Kh18N10T steel and "grade 20" steel are close to each other: conditional yield stress of 12Kh18N10T steel is about $\sigma 0.2 \approx 270$ MPa, while "grade 20" steel exhibits a yield plateau with an average stress level of $\sigma_y \approx 320$ MPa. At

Edelweiss Applied Science and Technology
ISSN: 2576-8484
Vol. 8, No. 6: 1554-1565, 2024
DOI: 10.55214/25768484.v8i6.2273

the same time, 12Kh18N10T steel is characterized by higher ultimate tensile strength (UTS) and better ductility properties.

Table 5
Mechanical properties of specimens from steel 20 and 12Kh18N10T steel, obtained from the parent metals tensile tests (mean values).

Material	Yield strength σ_y or $\sigma_{0.2}$, MPa	UTS σ_u, MPa	Ultimate uniform elongation δ_u, %	Elongation at break δ, %
Steel 20	321	398	13	15
12Kh18N10T steel	270	631	55	58

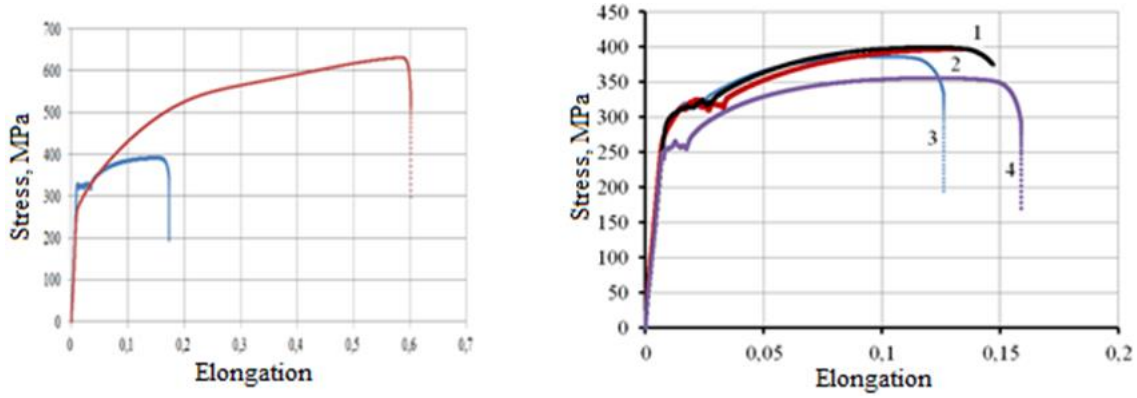

Figure 5.
Tensile diagrams for "grade 20" steel and 12Kh18N10T steel (a) and for dissimilar welds (b): 1 – without heat treatment, 2 – heat treatment with holding time of 1 hour at 650°C, 3 – 5 hours at 650°C, 4 – 25 hours at 650°C.

The stress-strain curve of specimens with welded joints (Figure 5b) exhibits several distinct regions. For the welded specimen without heat treatment (see Figure 5b, diagram 1), a linear section is observed on the stress-strain curve up to a stress of about 250 MPa, indicating that both steels and the weld seam are deforming elastically. At a stress of approximately 250 MPa, plastic deformation of the 12Kh18N10T steel begins, and at around 320 MPa, the diagram shows a yield plateau corresponding to "grade 20" steel. Following the yield plateau, a strain hardening region occurs, where both steels undergo elastoplastic deformation. After reaching the ultimate stress, the diagram shows a decline, after which the specimen fractures along the "grade 20" steel.

After heat treatment, the properties of the welded joints underwent certain changes. The stress-strain curves of the welded specimens after various heat treatment modes are presented in Figure 5b (diagrams 2–4). The diagrams indicate that under the thermal treatment conditions of 650°C (1 hour) and 650°C (5 hours), the strength characteristics of the welded specimens remained at their previous levels, with an increase in the ductility. However, with prolonged high-temperature exposure (650°C, 25 hours), there was a reduction in the ultimate tensile strength and yield strength of the welded joint due to the degradation of "grade 20" steel properties.

3.2. AE Data Analysis

Figures 6 and 7 show AE activity and the amplitudes of AE impulses obtained for defect-free specimens (without diffusion interlayers) (Figures 6a and 7a), specimens with thin interlayers up to 145 μm (Figures 6b and 7b), and specimens with medium-thickness interlayers up to 225 μm (Figures 6c and 7c). The patterns of AE data for specimens without defects and with diffusion interlayers do not have significant differences. During the elastic deformation stage and the initial stage of strain hardening, an increase in AE activity is observed, followed by an acoustic silence during the yield plateau, and a subsequent rise in AE activity during strain hardening. The presence of AE activity in

Edelweiss Applied Science and Technology
ISSN: 2576-8484
Vol. 8, No. 6: 1554-1565, 2024
DOI: 10.55214/25768484.v8i6.2273

the elastic region of "grade 20" steel is not typical, as AE sources associated with intense dislocation generation are absent in the elastic region. The authors [11, 12] have proposed that magnetoelastic processes occurring during deformation may influence these AE data. During the elastic deformation of ferromagnetic materials, the magnetoelastic effect is characterized by a monotonic, smooth change in mechanical stress leading to abrupt changes in the magnetic field intensity, which in turn results in the movement of domain walls—the boundaries between magnetic domains with different magnetization directions [13, 14].

However, in the localized region at a stress level of 300 MPa, close to the ultimate tensile strength of the ferritic phase, AE activity and the amplitudes of AE impulses for specimens with diffusion interlayers were higher than for the defect-free specimen. This effect is not clearly visible on the time-dependent curves, as at a constant strain rate, the period of stress increase from 290 to 310 MPa lasts for 1-2 minutes, while the total time from the beginning of loading to specimen failure exceeds one hour.

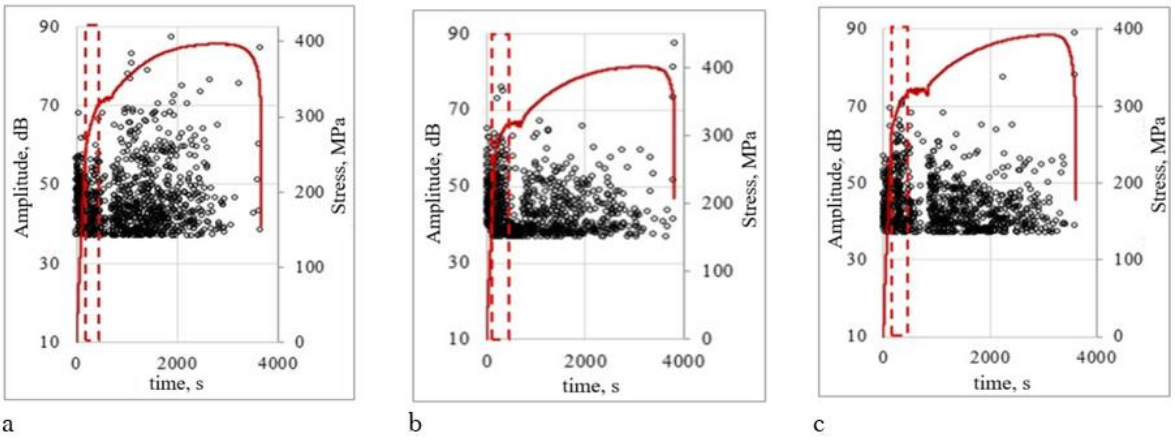

Figure 6.
The amplitudes of AE impulses vs. time for defect-free specimen (a), and specimens with diffusion interlayers thickness of 145 μm (b) and thickness of 225 μm (c).

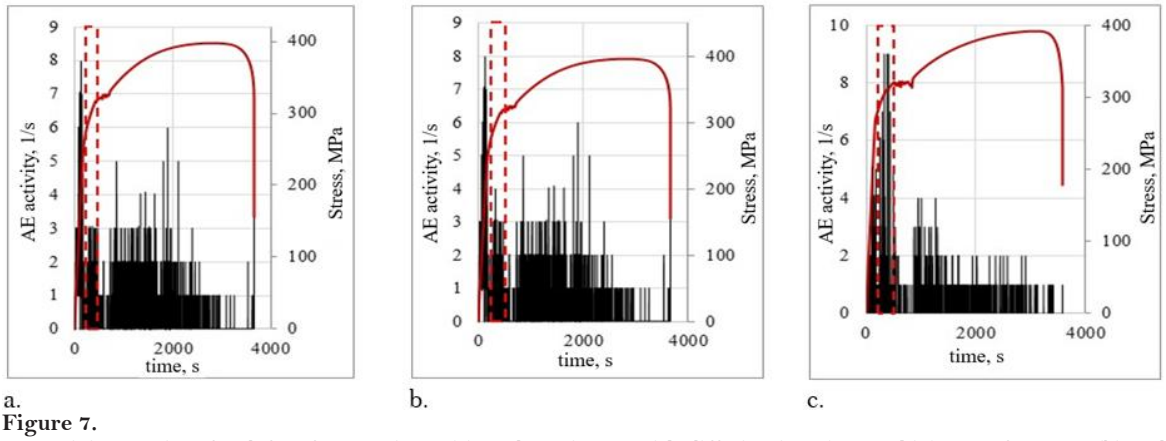

Figure 7.
AE activity vs. time for defect-free specimen (a), and specimens with diffusion interlayers thickness of 145 μm (b) and thickness of 225 μm (c).

For a more detailed analysis of AE parameters, the time-dependent curves shown in Figures 6 and 7 were transformed into dependencies of AE parameters vs. mechanical stress value (Figs. 8 and 9). In this form, the AE data correspond to the Dunnegan model [15]—during the elastic region, low AE

Edelweiss Applied Science and Technology
ISSN: 2576-8484
Vol. 8, No. 6: 1554-1565, 2024
DOI: 10.55214/25768484.v8i6.2273

impulse amplitudes and low AE activity are observed, followed by a sharp increase in AE impulse amplitudes during the plastic strain region.

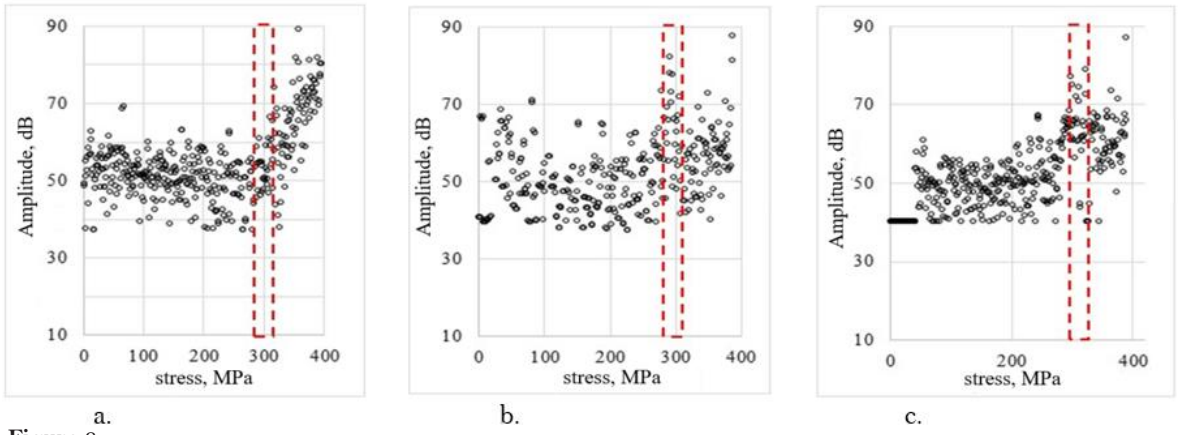

Figure 8.
AE amplitude vs. stress for defect-free specimen (a), and specimens with diffusion interlayers thickness of 145 μm (b) and thickness of 225 μm (c).

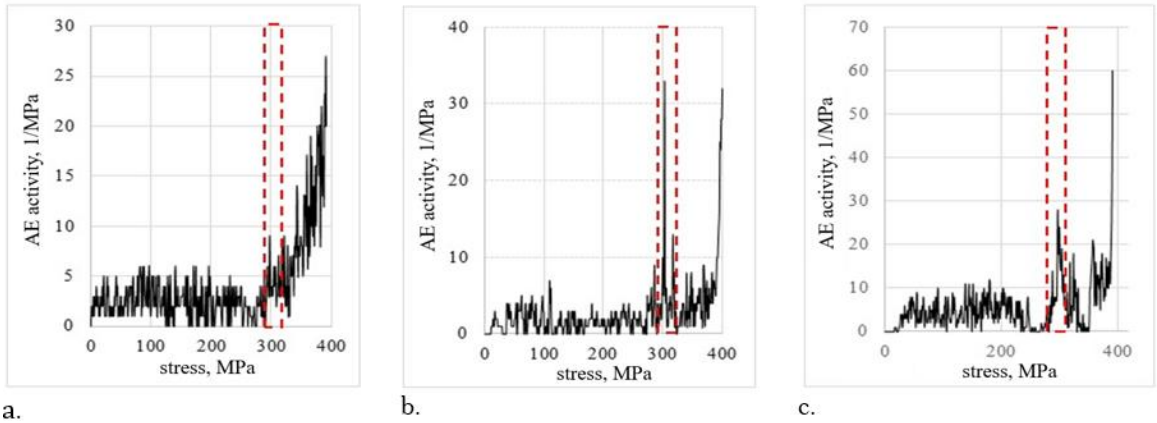

Figure 9.
AE activity vs. stress for defect-free specimen (a), and specimens with diffusion interlayers thickness of 145 μm (b) and thickness of 225 μm (c).

In addition to the overall similarities observed for defective specimens, specimen with diffusion interlayers show a pronounced local increase in AE impulse amplitudes and AE activity at a stress level of 300 MPa, corresponding to the ultimate tensile strength of the ferritic phase.

Edelweiss Applied Science and Technology
ISSN: 2576-8484
Vol. 8, No. 6: 1554-1565, 2024
DOI: 10.55214/25768484.v8i6.2273

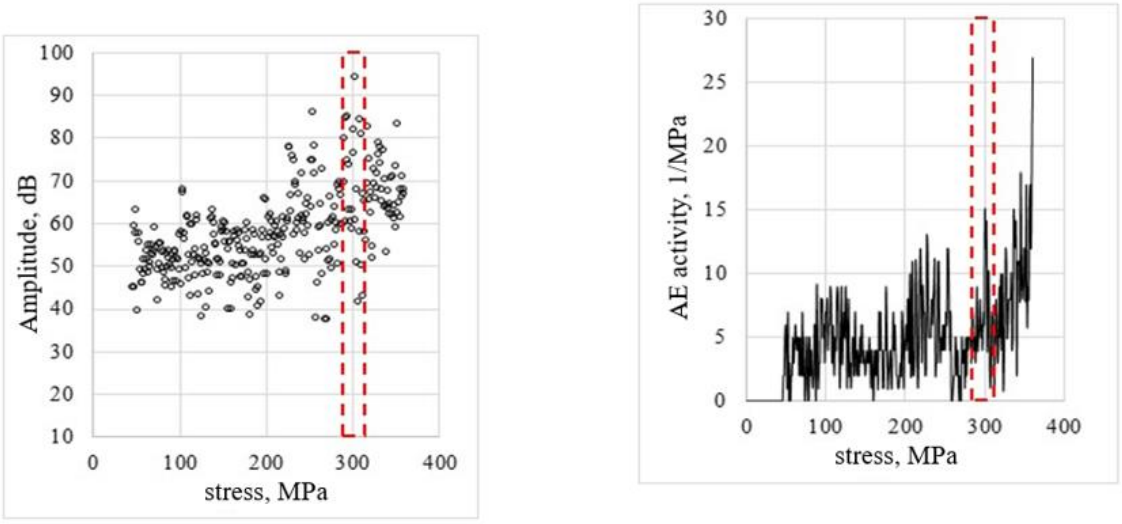

Figure 10.
AE data for the specimen of dissimilar weld with 600 μm diffusion interlayers, AE amplitudes (a) and activity (b) vs. stress value.

For the specimens subjected to prolonged heat treatment (held at 650°C for 25 hours), the characteristics of the AE data differ from the previous cases. In the strain hardening region, lower AE activity is observed compared to specimens with shorter heat treatment time, while the AE impulse amplitudes are 10-15 dB higher than in the previous cases (Figure 10). Such changes in AE data can be explained by microstructure changes in "grade 20" steel due to long-term heat treatment, leading to the removal of internal stresses, which in turn leads to lower AE activity. In addition, this heat treatment inevitably causes an increase in the ferrite grain size in the base metal structure, which leads to higher AE pulse amplitudes.

The increase in AE activity and the amplitude levels of AE impulses at a stress of 300 MPa in the specimen with the thickest interlayer is occurred weaker than in specimens with thinner interlayers. This phenomenon is presumably associated with a reduction in the soft interlayer constraint effect due to the increased thickness of the ferrite interlayer in specimens subjected to prolonged heat treatment [2, 16].

3.4. The Study of the AE Signal Frequency Spectrum

A more detailed analysis of AE data was carried out through the examination of the frequency spectrum of AE signals recorded under stresses range from 290 to 310 MPa.

Edelweiss Applied Science and Technology
ISSN: 2576-8484
Vol. 8, No. 6: 1554-1565, 2024
DOI: 10.55214/25768484.v8i6.2273

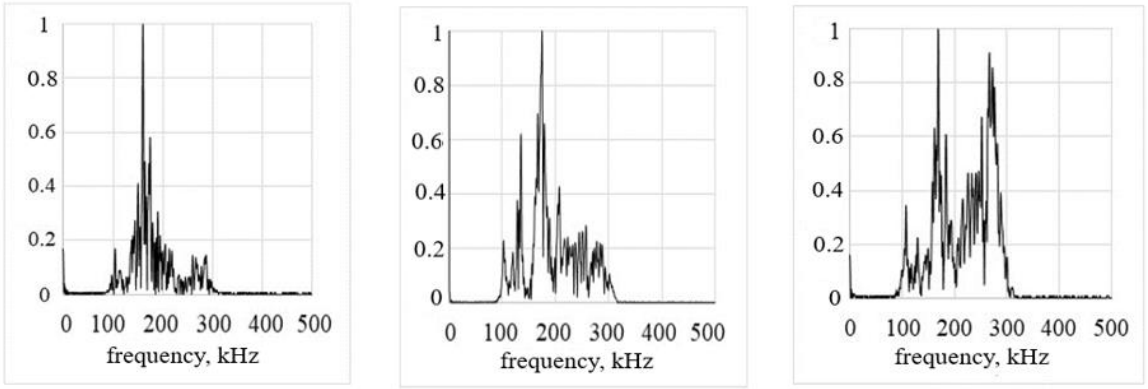

Figure 11.
Normalized frequency spectrum of AE for defect-free specimen (a), for specimens with diffusion interlayers thickness of 145 μm (b), and 600 μm (c).

Normalized frequency spectra of AE signals from the tests of defect-free specimen (Fig. 11a) and specimens with diffusion interlayers of different thickness (Fig. 11b-11c) are presented on the Fig. 11. The spectrum of the signal obtained from testing a defect-free specimen is narrowband, with a peak in the region of the sensor's resonant frequency. When testing specimens with diffusion interlayers, wideband frequency spectra are observed, and the width of the spectrum increases with the increase of the diffusion interlayer thickness. The median frequency (1), which corresponds to the center of mass of the spectrum [17], is traditionally used to characterize AE signal spectra:

$$\int_{f_l}^{f_{med}} S(f)df = \int_{f_{med}}^{f_u} S(f)df, \qquad (1)$$

where $S(f)$ – signal spectrum, f_u и f_l – upper and lower frequency.

The median frequency is an integral parameter that allows for the evaluation of overall changes in the frequency spectrum obtained from testing specimens with diffusion interlayers compared to defect-free specimens. For defect-free specimens, the characteristic median frequency lies in the range of 155-165 kHz, while for specimens with diffusion interlayers, the median frequency shifts to the right and typically falls within the range of 170-190 kHz.

4. Conclusions

The studies of welded joints of "grade 20" steel and steel 12Kh18N10T were carried out using the acoustic emission method. The data analysis revealed that for accurate data interpretation, it is necessary to analyze the dependence of AE parameters (AE activity and pulse amplitude values) on mechanical stress. This method of data presentation highlights clear differences in AE parameters in the elastic and elastic-plastic regions of the tensile diagram, as well as parameter characteristics related to the presence of diffusion interlayers in the structure of the dissimilar weld joint.

It was determined that the presence of diffusion interlayers in the dissimilar weld joint of "grade 20" steel carbon steel to 12Kh18N10T austenitic steel causes a local increase in AE activity and pulse amplitudes at a stress level of approximately 300 MPa, close to the tensile strength of the ferritic phase.

For specimens after long-time heat treatment (holding at 650°C for 25 hours) with a ferritic interlayer thickness of 600 μm, lower AE activity is recorded at the strain hardening stage compared to specimens with thinner interlayers, while AE pulse amplitudes are 10-15 dB higher than in previous cases. These changes in AE data can be explained by microstructure changes in "grade 20" steel due to long high-temperature exposure. The decrease in AE activity is attributed to the internal stress relief,

Edelweiss Applied Science and Technology
ISSN: 2576-8484
Vol. 8, No. 6: 1554-1565, 2024
DOI: 10.55214/25768484.v8i6.2273

while the increase in AE pulse amplitudes is due to the growth of the average ferritic grain size in "grade 20" steel.

Based on the analysis of acoustic emission (AE) signals, it has been established that the presence of diffusion interlayers within the structure of dissimilar welds can be identified by a local increase in AE activity and amplitudes under stress of 300 MPa close to the yield strength of the ferritic phase. Additionally, spectral characteristics such as median frequency and spectral entropy are useful for interlayers detection. Spectral parameters from specimens with diffusion interlayers show higher values compared to defect-free specimens.

Funding: The research was carried out at the expense of a grant from the Russian Science Foundation No. 23-29-00657, https://rscf.ru/project/23-29-00657/

References

[1] *V.D. Khodakov, D.V. Khodakov*, "Structure and mechanism of formation of dissimilar welded joints in nuclear power plant made of austenitic and pearlitic steels," Welding International, vol. 30, no. 12, pp. 935-940, 2016. DOI: 10.1080/09507116.2016.1157331

[2] *A.L. Goncharov, A.Yu. Marchenkov, E.V. Terentyev, I.E. Zhmurko, A.P Sliva*, "Study of structural non-homogeneity impact on mechanical properties of dissimilar weld joints of carbon steel 20 and corrosion-resistant austenitic 12Kh18N10T steel, " IOP Conference Series: Materials Science and Engineering, vol. 681, no. 012016, 2019. DOI: 10.1088/1757-899X/681/1/012016

[3] *A. V. Berezovsky, E. B. Votinova, and A. S. Smolentsev*, "The technology of arc welding of dissimilar steels, " Diagnostics, Resource and Mechanics of materials and structures, Iss. 5, p. 31–38, DOI: 10.17804/2410-9908.2023.5.031-038, 2023.

[4] *Mani Jayavelu, Srinivasan Kasi, Balasubramanian Visvalingam, Prasanna Nagasai Bellamkonda, Sudhakara Dara*, "Wear properties and microstructural characteristics of mild steel cladded with AISI 316L stainless steel using constant current gas metal arc welding process, " Materials Today: Proceedings, 2023, https://doi.org/10.1016/j.matpr.2023.05.060

[5] *V.G. Shmorgun, O.V. Slautin, V.P. Kulevich, A.I. Bogdanov, L.M. Gurevich, A.G. Serov*, "Influence of Nickel Content on the Formation of an Interaction Zone during Contact Melting of Titanium with Copper-Nickel Alloys," Metals **2024**, 14, 298. https://doi.org/10.3390/met14030298

[6] V.G. Shmorgun, A.I. Bogdanov, and V.P. Kulevich, "Formation of the Diffusion Coatings Structure on the Surface of the Fe–Cr–Al Alloy during Hot-Dip Aluminizing with Ultrasonic Impact," Metallurgist **67**, 1138–1145, 2023. https://doi.org/10.1007/s11015-023-01605-1

[7] *V.N. Gadalov, A.E. Gvozdev, A.G. Kolmakov, et al.* "Regularities of Structure Formation of Aluminum Powdered Particles Produced by Reactive Mechanical Alloying," Inorg. Mater. Appl. Res. **11**, 198–201, 2020. https://doi.org/10.1134/S2075113320010128

[8] *A. V. Ozolin et al* "Effect of tungsten nanoparticles on interaction of Sn-Cu-Co metallic matrices with diamond," 2021 IOP Conf. Ser.: Mater. Sci. Eng. 1155 012016 DOI: 10.1088/1757-899X/1155/1/012016

[9] *A.V. Berezovsky, E.B. Votinova, A.S Smolentsev*, "The technology of arc welding of dissimilar steels," Diagnostics, Resource and Mechanics of materials and structures, iss. 5, pp. 31–38, 2023.

[10] *Barat V.,Marchenkov A., Bardakov V., Balandin, T., Elizarov, S.*, Assessment of the Structural State of Dissimilar Welded Joints by the Acoustic Emission Method. Applied Sciences (Switzerland), 2022, 12(14), 7213 DOI: 10.3390/app12147213

[11] *Meysam Akbari, Mehdi Ahmadi*, "The application of acoustic emission technique to plastic deformation of low carbon steel," Physics Procedia, vol. 3, iss. 1, pp. 795-801, 2010 ISSN 1875-3892, https://doi.org/10.1016/j.phpro.2010.01.102

[12] *Frank P. Higgens, Steve H. Carpenter*, "Sources of acoustic emission generated during the tensile deformation of pure iron," Acta Metallurgica, vol. 26, iss. 1, pp. 133-139, 1978,ISSN 0001-6160, https://doi.org/10.1016/0001-6160(78)90209-2

[13] *Morrish, Allan H.* "The Physical Principles of Magnetism," The Institute of Electrical and Electronics Engineers, 680 p. Inc. 2001.

[14] *A.E. Lord, W.P. Mason, R.N. Thurston*, "Acoustic Emission," Physical Acoustics, Academic Press, vol. 11, pp. 289-353, 1975 ISSN 0893-388X, ISBN 9780124779112, https://doi.org/10.1016/B978-0-12-477911-2.50011-9.

[15] Ono, K. (2014). Acoustic Emission. In: Rossing, T.D. (eds) Springer Handbook of Acoustics. Springer Handbooks. Springer, New York, NY. https://doi.org/10.1007/978-1-4939-0755-7_30

[16] Terentyev, E.V., Zhgut, D.A., Gudenko, A.V. et al. Influence of the scale effect on the constraint effect in welded joints with soft interlayers. Int J Adv Manuf Technol **126**, 2357–2368 (2023). https://doi.org/10.1007/s00170-023-11287-3

[17] *A.Y. Vinogradov, D.L. Merson*, "The Nature of Acoustic Emission during Deformation Processes in Metallic Materials," *Low Temperature Physics*, vol. 44, no. 9, pp. 930-937, 2018. DOI: 10.1063/1.5052679

Edelweiss Applied Science and Technology
ISSN: 2576-8484
Vol. 8, No. 6: 1554-1565, 2024
DOI: 10.55214/25768484.v8i6.2273